Supplementary Materials and Methods

Animals

Duoxa$^{-/-}$ and gender-matched wt littermates were cohoused (3-5 animals/cage) in microisolator cages under SPF conditions [1]. Food and water were supplied ad libitum, with the latter including a supplemental dose of L-thyroxine to maintain euthyroidism of *Duoxa*$^{-/-}$ mice [2]. For experiments involving *Duoxa*-deficient mice, animals used were in a pure 129S6 genetic background, except for studies shown in Fig. S9 and S12 that employed mice backcrossed for ten generations into C57BL6 background. All of the latter were confirmed to be homozygous carriers of the G169D *Slc11a1* variant (rs47476426) genotyped using a HypCH4III endonuclease (New England Biolabs) restriction fragment length polymorphism. *Il22*$^{-/-}$, *Il23r*$^{-/-}$, and *RORgt*$^{-/-}$ mice (all in B6 background) have been described previously [3-5]. C57BL6 mice with distinct resident microbiota were purchased from Taconic Farms and Jackson Laboratory, respectively. For all studies, mice were used at 9-12 weeks of age. Studies were approved by the University of Michigan Institutional Animal Care and Use Committee (PRO-00004497 and PRO-00002436).

Mono-association of mice with SFB

GF mice were aseptically transferred to microisolator cages and housed in sterile laminar-flow hoods. Mice were orally gavaged with a freshly prepared suspension of frozen cecal material from SFB^{mono} mice [6] or GF controls. Tissues were collected one week following treatment. All mice remained bacteriologically sterile except for the presence of SFB (unculturable, positive gram-staining) in monocolonized mice.

Tissue collection

Animals were euthanized by isoflurane overdose. MLN, liver and spleen were harvested aseptically. Intestinal segments were collected from the duodenum (immediately following the

pylorus), jejunum (halfway between stomach and cecum), ileum (terminal portion), colon (midportion) and rectum. The isolated segments were opened longitudinally and rinsed thrice with PBS. Samples for nucleic acid extraction were snap frozen in liquid nitrogen. Samples for paraffin-embedding were fixed in 10% formalin. For cryosectioning, samples were snap-frozen in Tissue-Tek O.C.T. compound (Andwin Scientific, Woodland Hills, CA).

Histology and morphometric analysis

Serial 4 µm sections of formalin-fixed paraffin-embedded samples were stained with H&E. For morphometry, the terminal ileum was scored for height of villi and depth of crypts on transverse sections at 200× magnification (Figure S7). For each animal, mean values were determined from at least 10 well oriented villus-crypt units. To assess mucosal macrophage accumulation, sections were histochemically stained for F4/80 (clone A3-1; 1:200; Abcam ab6640) and counterstained with hematoxylin. Average F4/80-positive cell number per villus-crypt unit was determined by analyzing at least 20 villus-crypt units per animal.

Real-time reverse transcription PCR (RT-qPCR)

Total RNA was prepared using TRIzol reagent, treated with deoxyribonuclease and cleaned up on RNeasy spin columns (Qiagen). RNA was reverse transcribed with Superscript II (Life Technologies) using random hexamer priming. Concentration and purity of RNA preparations were determined on a NanoDrop ND-1000 UV spectrophotometer. PCR amplifications were performed using a C1000 Thermal Cycler (Bio-Rad) with SYBR Green dye (Molecular Probes, Carlsbad, CA) and Platinum Taq DNA polymerase (Invitrogen). Each reaction was performed in triplicates with the following conditions: 1 min at 95°C, 40 cycles of 10 s at 95°C and 1 min at 65°C. Amplification specificity was confirmed by melting curve analysis of products. Gene expression of host genes was normalized to *Hprt1* mRNA. Expression stability of *Hprt1* was confirmed for all samples by comparison with a second house keeping gene, *Polr2a*. The

expression of SFB genes was normalized to SFB-specific 16S rRNA. Primer sequences are listed in Supplementary Table S15.

Microarray-based gene expression profiling

Total RNA was prepared using TRIzol reagent, treated with deoxyribonuclease and cleaned up on RNeasy spin columns (Qiagen). RNA integrity numbers (RIN) were determined using a Bioanalyzer instrument (Agilent Technologies) and ranged from 9.2 to 9.6 (mean: 9.5) with 28S/18S ratios between 1.8 and 1.9. Target labeled cRNA were hybridized to GeneChip Mouse Genome 430 2.0 arrays (Affymetrix). Data were normalized with the RMA procedure using the affy package of Bioconductor implemented in the R statistical language. The dataset is accessible from the NCBI's Gene Expression Omnibus through series GSE60933. For GSEA [7], genes regulated by SFB colonization were selected from GSE18348 [8] based on 2.5-fold upregulation or 2-fold downregulation (unadjusted P<.05) in the comparisons of SFB^{mono} mice with GF mice and cohoused B6-Jax (+B6-Tac) with B6-Jax mice, respectively. Genes significantly up- or downregulated in the non-affected ilea of patients with cCD compared to ilea of healthy controls have been reported by Haberman et al. [9] (GSE57945). Genes were ranked by geometric means of expression ratios of cohoused *Duoxa*$^{-/-}$ and wt controls. Significance of the enrichment score was calculated from 1000 random, size-matched gene set permutations.

DNA isolation and 16S qPCR

Genomic DNA was extracted from tissue samples as described [10]. Phyla-specific PCR primers (Table S15) were used under validated conditions [11-14]. Relative bacterial loads were compared using the $2^{-\Delta\Delta Ct}$ method by normalizing 16S signal to the host DNA amplification signal.

16S rRNA in situ hybridization and immunostaining of tissue sections

For staining of frozen sections, thawed 8 µm sections were briefly fixed in 4% freshly prepared

formaldehyde for 5 min, washed twice in PBS, and then blocked with 20% donkey serum in PBS. Primary antibodies used were a pan-DUOX antiserum (1:1,000) [15] or normal rabbit IgG (control; Santa Cruz Biotechnology, Santa Cruz, CA), an anti-*Salmonella* Typhimurium LPS monoclonal antibody (clone 1E6; 1:1,000) (GeneTex), and rat anti-E-cadherin (1:2,000) (Life Technologies). The staining was developed using Alexa Fluor-conjugated secondary antibodies (Life Technologies) and DNA counterstained with DAPI.

Sequential in 16S rRNA situ hybridization and immunodetection followed protocols outlined previously in detail [16]. Briefly, Carnoy's solution-fixed sections were hybridized in a humid chamber for 2 hours at 50°C with 5 ng/µl Alexa Fluor 488 labeled oligonucleotide SFB1008 (AF488-5'- GCGAGCTTCCCTCATTACAAGG-3') [11] in a formamide-free hybridization buffer. Following washes in hybridization buffer and PBS, sections were blocked and stained for DUOX protein as described above.

Enteric *Salmonella* Typhimurium infection model

Salmonella enterica serovar Typhimurium (strain SL1344) was grown at 37°C with shaking (150 rpm) in Luria-Bertani (LB) broth containing 100 µg/ml streptomycin. In the streptomycin-pretreated model [17], mice in 129S6 background were given 20 mg streptomycin orally followed 24 hours later by oral gavage with 10^7 cfu S. Typhimurium (1 OD_{600} ~ $6x10^8$ cfu/ml) in Hepes buffer (100 mM, pH 8.0) or with sterile buffer alone. In the thyphoid model, mice in C57BL6 background received 10^7 cfu S. Typhimurium by oral gavage without prior antibiotic pretreatment. Mice were euthanized 24 hours following infection. Livers were removed aseptically followed by collection of intestinal content from ileum, cecum, and colon. All samples were weighed and homogenized in 4°C cold PBS/0.1% Triton X-100. Cfu were determined by culturing serial dilutions on LB agar plates with 100 µg/ml streptomycin.

In vivo intestinal permeability assay

Intestinal permeability was assessed by measuring the enteral uptake of fluorescein isothiocyanate-conjugated dextran (FD4, 4 kDa, Sigma) [18]. Serum was obtained four hours after gavage with FD4 (0.6 mg per gram body weight). Serum FD4 levels were determined by fluorometry (ex/em, 490/530 nm) using standards serially diluted in mouse serum.

Ileal enteroid culture

The enteroid culture method was modified from the study by Sato et al. [19] The excised mouse ileum (~6 cm) was opened longitudinally, rinsed with PBS, then incubated in ice-cold PBS containing 3 mM EDTA for 30 min at 4°C. After manual shaking for 30 sec, the tissue was moved to fresh cold PBS and shaken for 2 min. The tissue fragments were allowed to settle and the supernatant was collected and passed through a 70-μm cell strainer to remove tissue fragments. Crypts were separated from suspended single cells by centrifugation at 150 g (2 min). The crypt pellet was resuspended with Matrigel (BD Bioscience) for seeding into 24 well plates (50 μl drop per well). After polymerization of the Matrigel, 0.5 ml culture medium composed of advanced DMEM/F12 supplemented with Hepes (10mM), N2-supplement (1:100), B-27 supplement (1:50), L-glutamine (1:100), penicillin/streptomycin (1:100), 500 ng/ml R-spondin1, 100 ng/ml noggin, 50 ng/ml Wnt-3a and 100 ng/ml epidermal growth factor was added (all from Life Technologies). The media and growth factors (except for Wnt-3a) were changed every 4 days. For passage at 7–10 days post-plating, wells were rinsed twice with ice-cold PBS. Matrigel containing the enteroids was resuspended in PBS and passed once through a 30 gauge needle. Enteroid fragments were pelleted at 200 g (1 min), washed once with ice-cold DMEM/F12, centrifuged again, and resuspended in Matrigel for plating.

Enteroids were stimulated by incubation in growth medium containing either recombinant murine IL-22 (50 ng/ml) or TNFα (60 ng/ml) (R&D Systems) for 18 hours. For immunostaining, washed enteroids were fixed in 1% freshly prepared formaldehyde (5 min), washed again, and

snap frozen in O.C.T. compound. For mRNA expression studies, culture medium was aspirated and the matrigel drop containing enteroids directly homogenized in TRIzol for subsequent RNA extraction.

DSS-induced intestinal inflammation model

To induce intestinal inflammation by dextran sulfate sodium salt (DSS), cohoused *Duoxa*$^{-/-}$ and wt littermates received drinking water with 3% DSS (36–50 kDa; MP Biomedicals) (refreshed daily). To test whether DUOX status affects the extent of epithelial damage and/or epithelial wound healing in this model, mice were exposed to DSS for seven days, followed by one day on regular drinking water to initiate epithelial restitution. The mice were checked each day for morbidity and their weights were recorded. In vivo permeability assay was performed as described above (*in vivo intestinal permeability assay*). Weight loss and recovery were indistinguishable between *Duoxa*$^{-/-}$ and wt mice exposed to repeat DSS cycles (Figure S10).

Colonization of mice with healthy and dysbiotic human fecal microbiota

Since mucosal dysbiosis in CD patients is not typically reflected by pronounced shifts in the microbial composition in the lumen [24], dysbiotic fecal samples were obtained from patients with active ulcerative colitis (dysbiosis at the family/phylum level confirmed by Illumina 16S rRNA sequencing; data not shown). Frozen stool samples from patients and healthy control donors were resuspended under anaerobic conditions and used to infect individual GF mice by gavage. Samples from the proximal colon were analyzed two weeks following microbial challenge.

Western blotting

Tissue samples were homogenized in Tissue Protein Extraction Reagent (T-PER, Thermo Scientific) containing a cocktail of protease inhibitors (Complete; Roche Applied Science) and incubated for 1 h at 4°C. The lysates was centrifuged 15 min at 10,000 rpm and concentration of

total soluble protein determined using the bicinchoninic acid method (BCA; Life Technologies). Equal amounts of solubilized proteins were diluted 3:1 in 4x reducing Laemmli buffer (BioRad) before loading and separation by SDS-PAGE electrophoresis. DUOX proteins were detected with pan-DUOX antibody (1:2,000) [15] and β-actin was detected as loading control (mAb C4; Santa Cruz Biotechnologies). For densitometry of bands, average density profile plots for individual lanes were generated and the peak areas above background level measured using the wand tool in ImageJ software [20].

Statistics

Log-transformed expression data from unpaired groups were analyzed using Welch's t-test (multiple comparisons adjustment: Bonferroni) or with one-way ANOVA and Bonferroni post-hoc tests. The Wilcoxon matched-pairs signed-rank test was used to test for differences between genotype groups in mixed housing experiments. Each cage was analyzed as a pair of the means obtained in *Duoxa*$^{-/-}$ and cohoused wt littermates (n=2-3 mice per genotype and cage). Data were analyzed using GraphPad Prism 6.0 (San Diego, CA).

Supplementary References

1. Grasberger H, El-Zaatari M, Dang DT, et al. Dual oxidases control release of hydrogen peroxide by the gastric epithelium to prevent Helicobacter felis infection and inflammation in mice. Gastroenterology 2013;145:1045-54.
2. Grasberger H, De Deken X, Mayo OB, et al. Mice deficient in dual oxidase maturation factors are severely hypothyroid. Mol Endocrinol 2012;26:481-92.
3. Zheng Y, Valdez PA, Danilenko DM, et al. Interleukin-22 mediates early host defense against attaching and effacing bacterial pathogens. Nat Med 2008;14:282-9.
4. Cox JH, Kljavin NM, Ota N, et al. Opposing consequences of IL-23 signaling mediated by innate and adaptive cells in chemically induced colitis in mice. Mucosal Immunol 2012;5:99-109.
5. Eberl G, Marmon S, Sunshine MJ, et al. An essential function for the nuclear receptor RORgamma(t) in the generation of fetal lymphoid tissue inducer cells. Nat Immunol 2004;5:64-73.
6. Umesaki Y, Okada Y, Matsumoto S, et al. Segmented filamentous bacteria are indigenous intestinal bacteria that activate intraepithelial lymphocytes and induce MHC class II molecules and fucosyl asialo GM1 glycolipids on the small intestinal epithelial cells in the ex-germ-free mouse. Microbiol Immunol 1995;39:555-62.
7. **Subramanian A, Tamayo P,** Mootha VK, et al. Gene set enrichment analysis: a knowledge-based approach for interpreting genome-wide expression profiles. Proc Natl Acad Sci U S A 2005;102:15545-50.
8. **Ivanov, II, Atarashi K,** Manel N, et al. Induction of intestinal Th17 cells by segmented filamentous bacteria. Cell 2009;139:485-98.
9. Haberman Y, Tickle TL, Dexheimer PJ, et al. Pediatric Crohn disease patients exhibit specific ileal transcriptome and microbiome signature. J Clin Invest 2014;124:3617-33.
10. Gillilland MG, 3rd, Erb-Downward JR, Bassis CM, et al. Ecological succession of

bacterial communities during conventionalization of germ-free mice. Appl Environ Microbiol 2012;78:2359-66.

11. Snel J, Heinen PP, Blok HJ, et al. Comparison of 16S rRNA sequences of segmented filamentous bacteria isolated from mice, rats, and chickens and proposal of "Candidatus Arthromitus". Int J Syst Bacteriol 1995;45:780-2.
12. Bacchetti De Gregoris T, Aldred N, Clare AS, et al. Improvement of phylum- and class-specific primers for real-time PCR quantification of bacterial taxa. J Microbiol Methods 2011;86:351-6.
13. Matsuda K, Tsuji H, Asahara T, et al. Sensitive quantitative detection of commensal bacteria by rRNA-targeted reverse transcription-PCR. Appl Environ Microbiol 2007;73:32-9.
14. Huijsdens XW, Linskens RK, Mak M, et al. Quantification of bacteria adherent to gastrointestinal mucosa by real-time PCR. J Clin Microbiol 2002;40:4423-7.
15. De Deken X, Wang D, Many MC, et al. Cloning of two human thyroid cDNAs encoding new members of the NADPH oxidase family. The Journal of biological chemistry 2000;275:23227-33.
16. Johansson ME, Hansson GC. Preservation of mucus in histological sections, immunostaining of mucins in fixed tissue, and localization of bacteria with FISH. Methods Mol Biol 2012;842:229-35.
17. **Grassl GA, Valdez Y,** Bergstrom KS, et al. Chronic enteric salmonella infection in mice leads to severe and persistent intestinal fibrosis. Gastroenterology 2008;134:768-80.
18. Napolitano LM, Koruda MJ, Meyer AA, et al. The impact of femur fracture with associated soft tissue injury on immune function and intestinal permeability. Shock 1996;5:202-7.
19. Sato T, Vries RG, Snippert HJ, et al. Single Lgr5 stem cells build crypt-villus structures in vitro without a mesenchymal niche. Nature 2009;459:262-5.

20. Schneider CA, Rasband WS, Eliceiri KW. NIH Image to ImageJ: 25 years of image analysis. Nat Methods 2012;9:671-5.

21. **Kuwahara T, Ogura Y,** Oshima K, et al. The lifestyle of the segmented filamentous bacterium: a non-culturable gut-associated immunostimulating microbe inferred by whole-genome sequencing. DNA Res 2011;18:291-303.

22. Pamp SJ, Harrington ED, Quake SR, et al. Single-cell sequencing provides clues about the host interactions of segmented filamentous bacteria (SFB). Genome Res 2012;22:1107-19.

23. Reimand J, Arak T, Vilo J. g:Profiler--a web server for functional interpretation of gene lists (2011 update). Nucleic Acids Res 2011;39:W307-15.

24. Gevers D, Kugathasan S, Denson LA, et al. The treatment-naive microbiome in new-onset Crohn's disease. Cell Host & Microbe 2014;15:382-392

Author names in bold designate shared co-first authors.

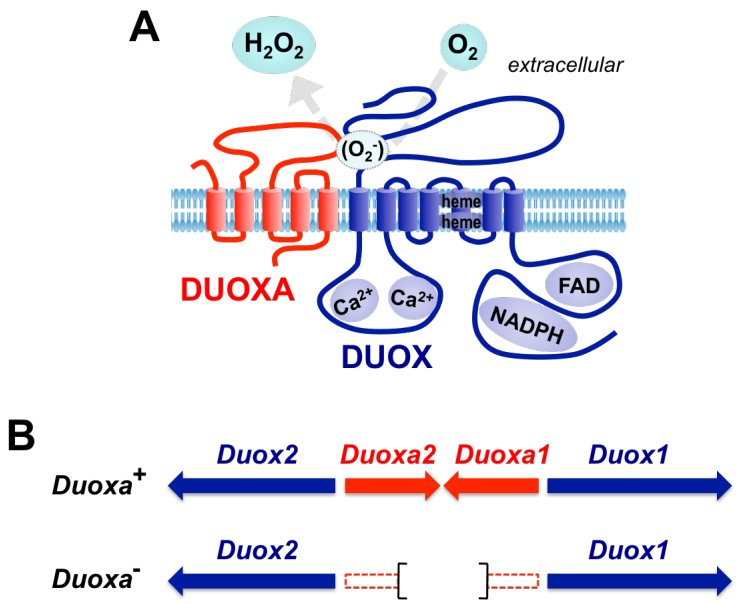

Supplementary Figure S1. Topology model of the DUOX/DUOXA complex and gene targeting strategy in *Duoxa*-deficient mice. (*A*) Topology model depicting the heterodimeric structure of a functional DUOX enzyme complex. (*B*) Arrangement of DUOX and DUOXA subunit genes on mouse chromosome 2 and targeting strategy to disrupt function of DUOX enzymes. *Duoxa*$^+$, wt allele; *Duoxa*$^-$, *Duoxa*-deficient allele.

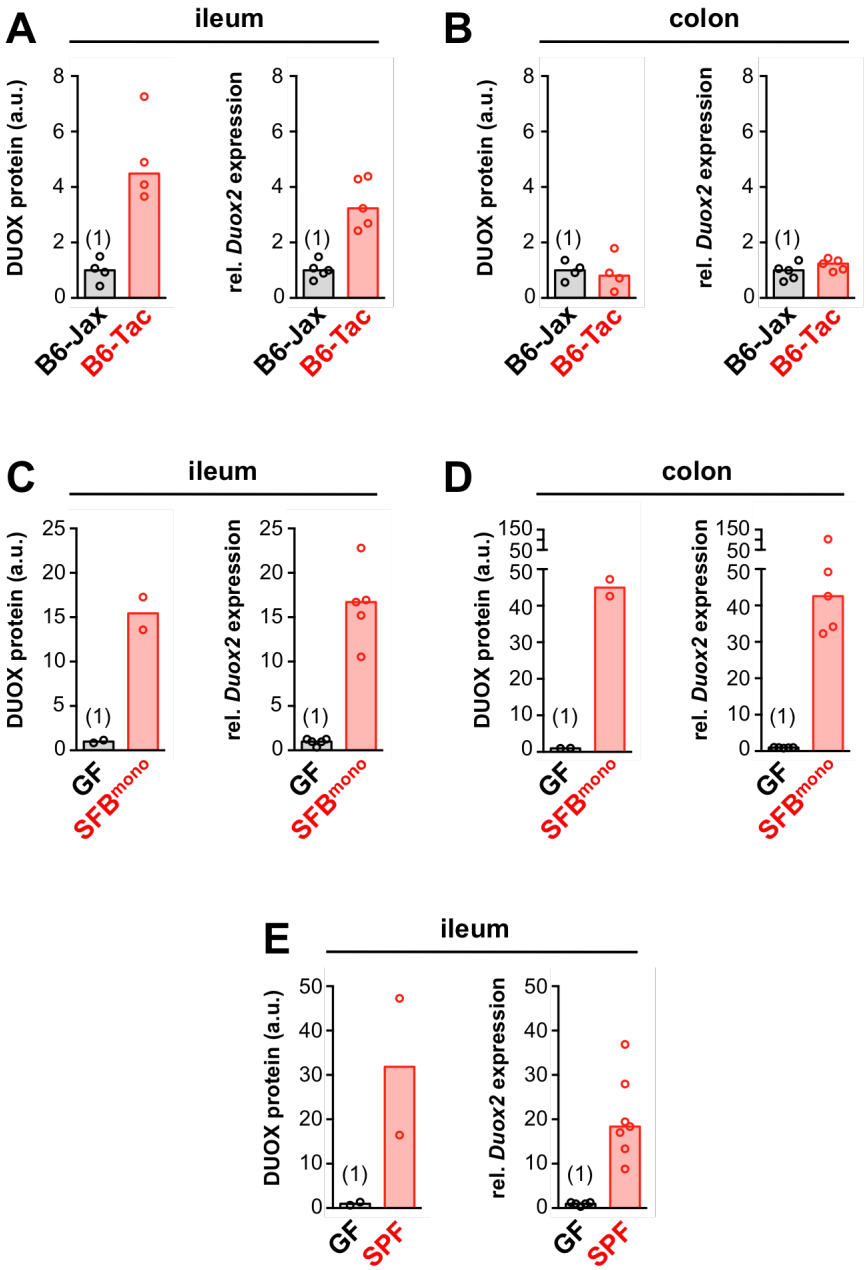

Supplementary Figure S2. Correspondence of DUOX protein expression with relative *Duox2* mRNA expression in mice associated with distinct microbiota. Relative DUOX protein expression was determined by densitometry of Western blots depicted in Figures 1 and 2 using ImageJ [20]. *a.u.*, arbitrary densitometric units.

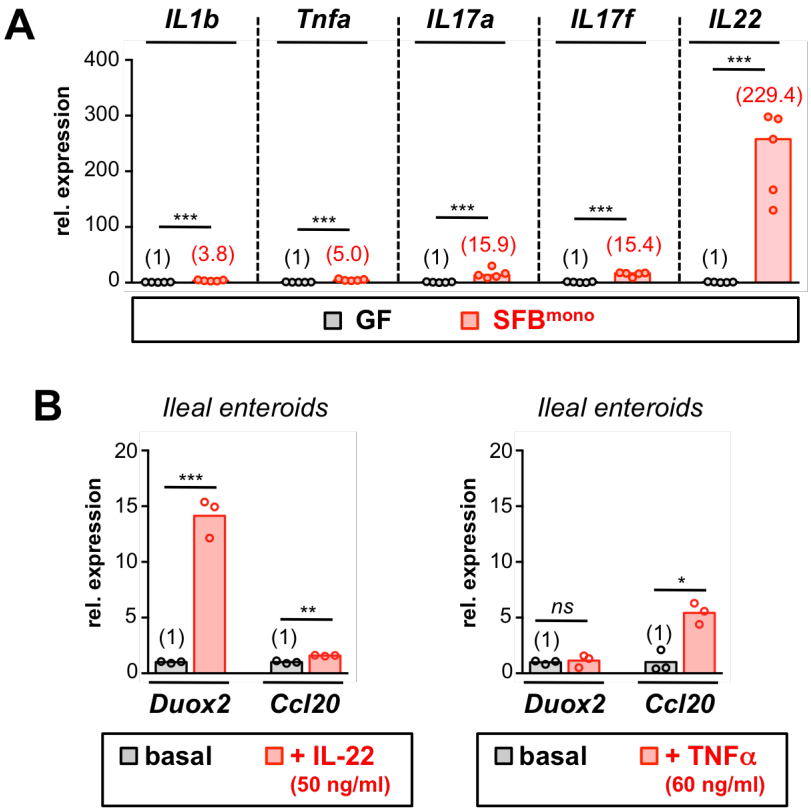

Supplementary Figure S3. (*A*) Induction of cytokines in the ileum of mice monocolonized for one week with SFB. *GF*, germ-free controls. (*B*) Ileal enteroids were treated for 18 hours with cytokines at the indicated concentration. Recombinant IL-22 but not TNFα is sufficient to robustly induce *Duox2* in vitro. ***, *P*<.001; **, *P*<.01; *, *P*<.05; *ns*, *P*>.05.

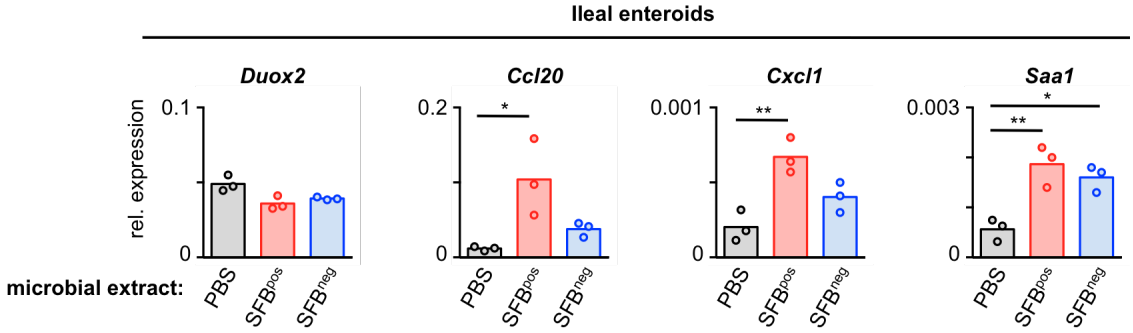

Supplementary Figure S4. Sterile microbial extracts do not induce *Duox2* expression in ileal enteroids. Sonicates of cecal contents of B6-Jax (SFB^{neg}) and B6-Tac (SFB^{pos}) mice were sterile-filtered (0.2 μm) and added to ileal enteroids cultured in complete growth medium (20 mg original wet weight/ml medium). Expression of *Duox2*, *Ccl20*, *Cxcl1*, and *Saa1* were evaluated after exposure for 16 hours. *, *P*<.05; **, *P*<.01.

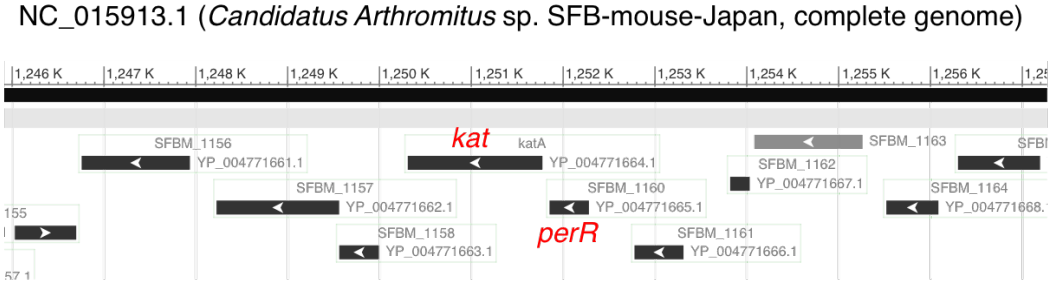

Supplementary Figure S5. Putative *perR-kat* operon in the SFB genome. Region of the SFB genome depicting the location of the *kat* (catalase) gene preceded by a putatively H_2O_2-sensitive transcriptional repressor (putative *perR*; *fur*-homolog sequence). This arrangement suggests a *perR-kat* operon for H_2O_2-induced derepression of *kat* providing a rationale for the observed DUOX2-dependent induction of SFB-*kat* in vivo.

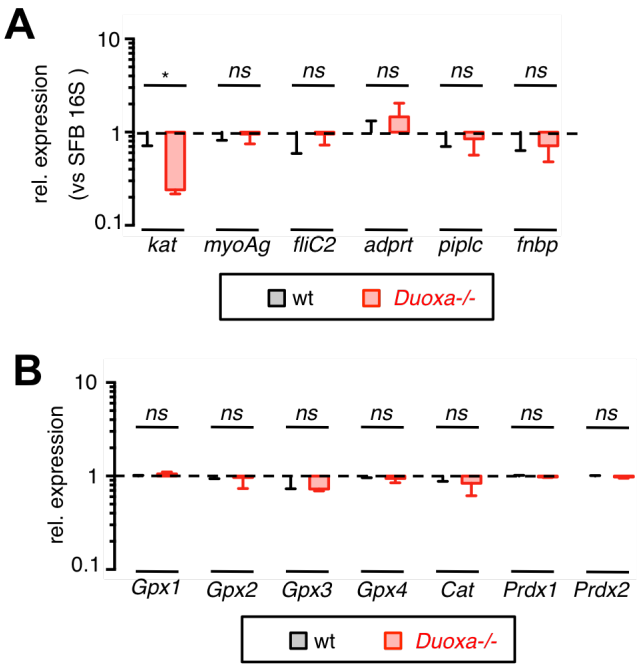

Supplementary Figure S6. Effect of DUOX status on anti-oxidative gene expression in ileal mucosa and mucosa-associated SFB. (*A*) Relative gene expression in mucosa-adherent SFB. *kat*, catalase (SFBM_1159); *myoAg*, myosin-crossreactive antigen-like (SFBM_0327); *fliC2*, flagellin (SFBM_0642); *adprt*, adenin-phosphoribosyltransferase homolog (SFBSU_007G84); *piplc*, phosphoinositide phospholipase C homolog (SFBM_0755); *fnbp*, fibronectin-binding protein (SFBM_0986). Except for *kat*, genes were selected based on a putative role in SFB-epithelial interaction [21,22]. (*B*) Relative ileal expression of antioxidant enzymes in DUOX intact (wt) vs DUOX deficient (*Duoxa*$^{-/-}$) mice. Values represent mean±SEM of n=3 independent expression ratios (intra-cage comparisons). *, *P*<.05; *ns*, *P*>.05.

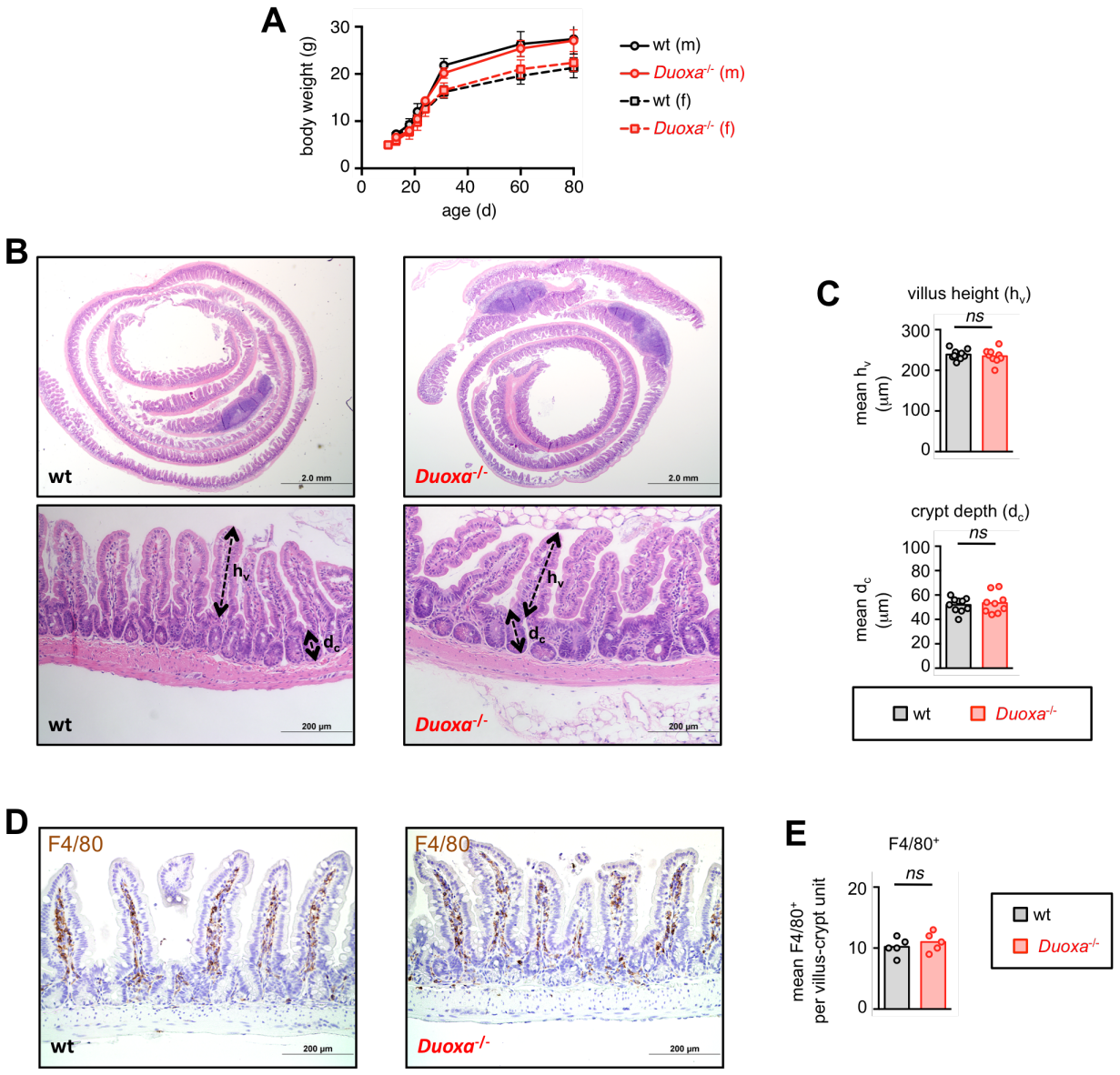

Supplementary Figure S7. Absence of DUOX activity in SPF mice does not lead to spontaneous intestinal inflammation. (*A*) Body weight gain of *Duoxa*$^{-/-}$ animals and wt littermates. Values indicate mean±SD of n=17-22 mice per group. *m*, males; *f*, females. (*B*) Exemplar hematoxylin and eosin stained sections of the small intestine of wt and *Duoxa*$^{-/-}$ littermates. Arrows in lower panels (20x objective magnification; ileum) indicate method of measurement of the height of villi (h_v) and depth of crypts (d_c). (*C*) Data show mean h_v and d_c values of wt (n=10) and *Duoxa*$^{-/-}$ (n=9) littermates. All mice were males, between 11-13 weeks of age. (*D*) Exemplar histochemical staining for the macrophage marker F4/80. Shown are transverse sections of the ileal mucosa of a wt and *Duoxa*$^{-/-}$ littermate pair. (*E*) Average number of F4/80-positive cells per villus-crypt unit. Values were determined by counting positive cells of at least 10 well-oriented villus-crypt units per animal. *ns*, *P*>.05.

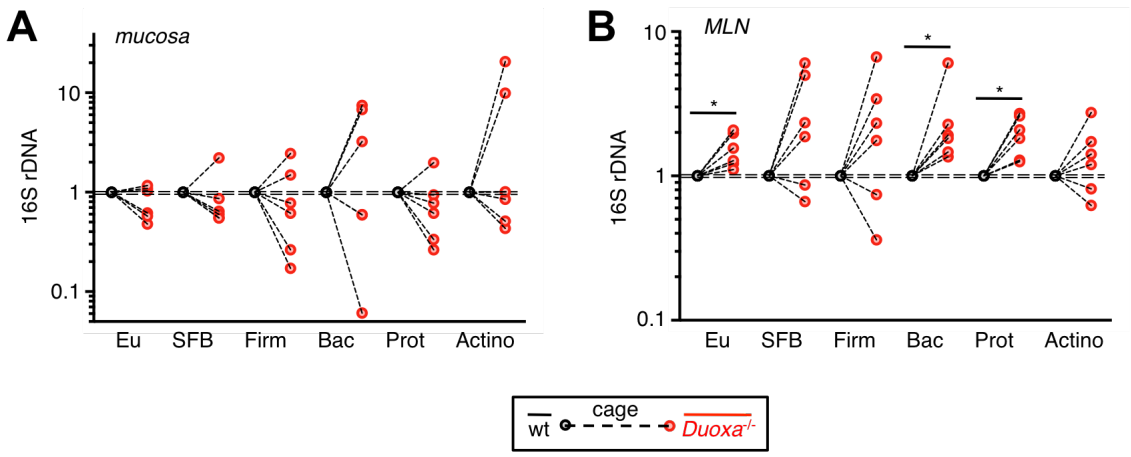

Supplementary Figure S8. Effect of DUOX status on bacterial DNA level in ileal mucosa and MLN. Relative level of group-specific 16S rDNA in ileal (*A*) and MLN (*B*) samples from *Duoxa*$^{-/-}$ and cohoused littermate controls. Dashed lines connect mean bacterial DNA level of *Duoxa*$^{-/-}$ and wt mice in intra-cage comparisons. For comparison between cages/litters, relative amounts were normalized within each cage (level in wt animals set to 1). *Eu*, eubacteria; *Firm*, Firmicutes; *Bac*, Bacteroidetes; *Prot*, Proteobacteria; *Actino*, Actinobacteria. *, *P*<.05, two-sided Wilcoxon matched-pairs signed rank test.

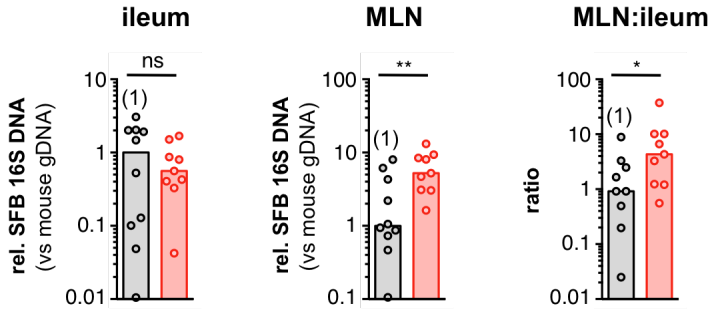

Supplementary Figure S9. Effect of DUOX status on bacterial DNA level in ileal mucosa and MLN in B6 mice. Relative level of 16S rDNA in ileal mucosal and MLN samples from *Duoxa*$^{-/-}$ and wt littermates in B6 genetic background. Mice from different litters were cohoused (mixed genotypes) after weaning. Bedding was mixed weekly between cages. Relative SFB 16S DNA level in MLN and ileal mucosa were determined in three months old mice by qPCR and normalized relative to the tissue genomic DNA level (mean level in wt mice set to 1). *ns*, *P*>.05; *, *P*<.05; **, *P*<.01; Mann-Whitney test.

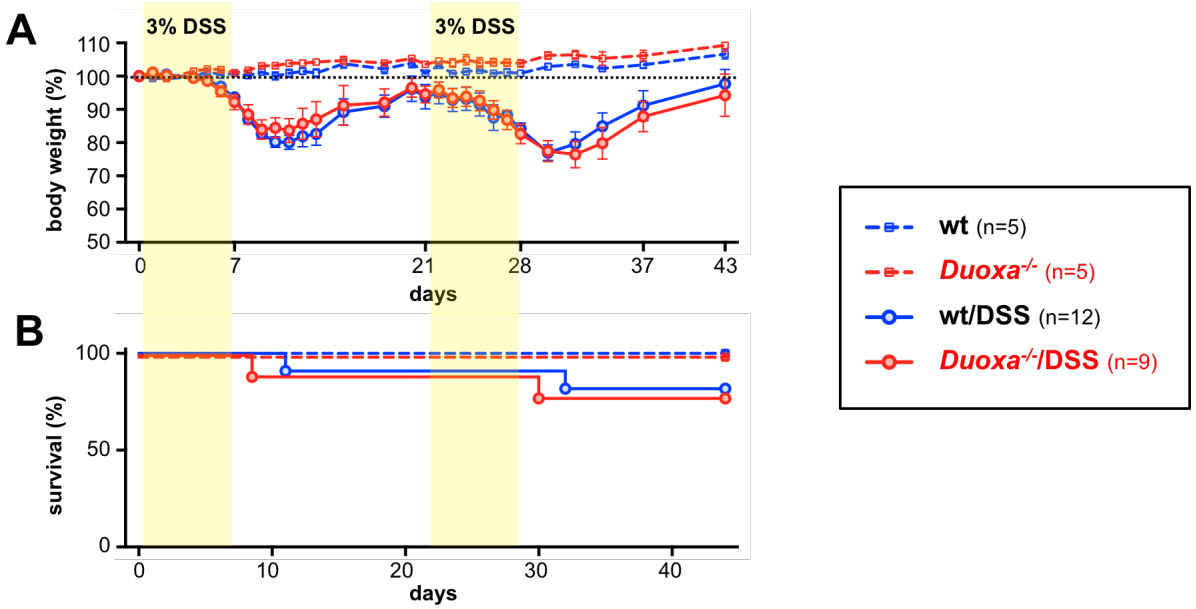

Supplementary Figure S10. Body weight change and survival in the DSS-induced intestinal inflammation model. Three months old mice (male 129S6) were treated with 7-day cycles of 3% DSS in drinking water followed by 14 days recovery period on regular drinking water. DSS-treated *Duoxa*$^{-/-}$ and wt mice did not differ in body weight change (*A*) or survival rate (*B*). Body weight data represent mean±SEM.

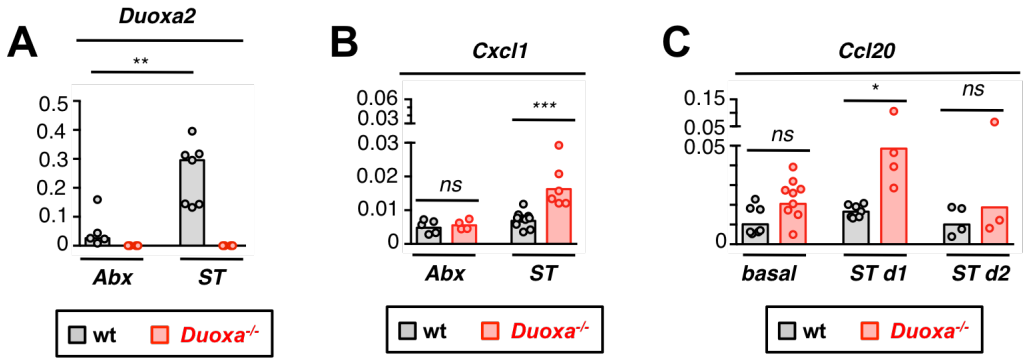

Supplementary Figure S11. Acute enteral *Salmonella* Typhimurium (*ST*) infection model. (*A*) Induction of *Duoxa2* expression in the ileum 24 hours following enteral infection with *ST*. *Abx*, sham-infected animals pretreated with streptomycin. (*C*, *D*) Ileal expression of epithelial chemokines *Cxcl1* and *Ccl20* during acute ST infection. ***, P<.001; **, *P*<.01; *, *P*<.05. Data were log-transformed before analysis to approximate Gaussian distribution. Bars indicate the geometric means.

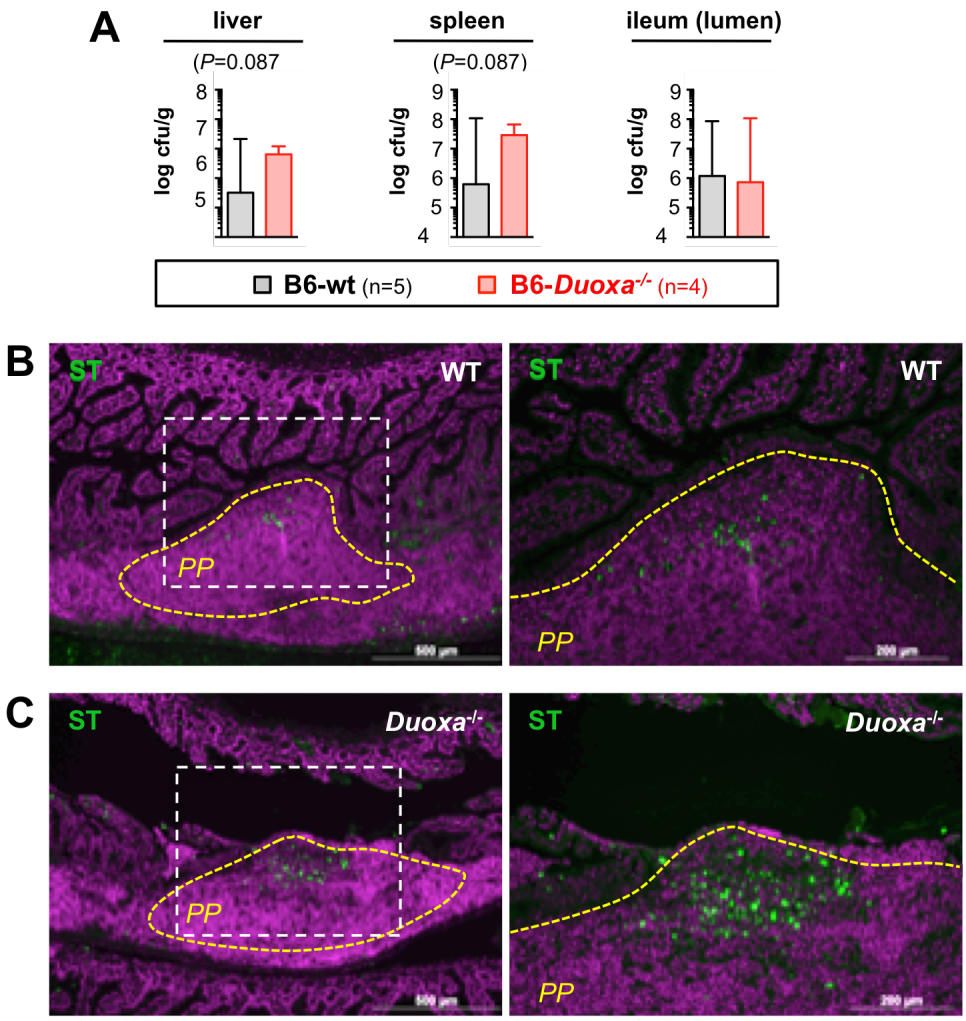

Supplementary Figure S12. Typhoid model of acute enteral *Salmonella* Typhimurium (*ST*) infection. B6 *Duoxa*$^{-/-}$ and wt littermates (10 generation of backcrossing onto C57BL/6 background; all homozygous for the G169D *Slc11a1* mutant) were orally infected with 1.5x10^{7} cfu ST without antibiotic conditioning. (*A*) Systemic dissemination (liver, spleen) and ileal colonization 48 h following infection. Data represent geometric means±95% CI. (*B*) Detection of ST within ileal Peyer's 48 h following oral gavage with ST. Indirect Immunofluorescence detection of ST-specific lipopolysaccharide (mAb clone 1E6; 1:1,000; Genetex; *green*). *Purple*, DNA counterstained with DAPI.

adj. *P*	GO#	GO term
9.18E-06	GO:0006952	defense response
2.34E-05	GO:0009611	response to wounding
2.88E-05	GO:0006954	inflammatory response
6.34E-04	GO:0006955	immune response

Supplementary Figure S13. Functional enrichment analysis of genes affected by DUOX status. Genes upregulated in *Duoxa*$^{-/-}$ mice (n=99 genes with mean >1.4 fold vs cohoused littermate controls) were tested for enrichment within the Biological Process terms subset of the Gene Ontology database using the g:GOSt program [23]. Listed *P* values are adjusted for multiple comparisons using the Bonferroni method.

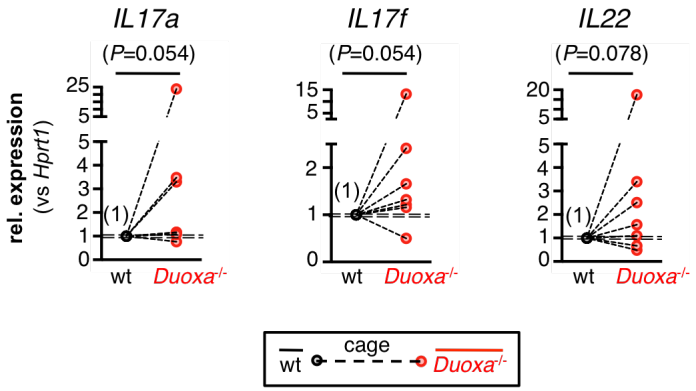

Supplementary Figure S14. Ileal expression of IL-17/22 cytokines. Mean expression in *Duoxa*$^{-/-}$ animals is plotted relative to the mean in co-housed wt littermates (set to 1). **, *P*<.01; two-sided Wilcoxon matched-pairs signed rank test.

Supplementary Table S15

qPCR primers

mouse mRNA-specific primers

name	5'-3' sequence	gene
DUOXA2-F	GCCTGGCTTTGCTCACCA	*Duoxa2*
DUOXA2-R	GAGGAGGAGGCTCAGGAT	
DUOXA1-F	CATCACCCTCACAGGCACC	*Duoxa1*
DUOXA1-R	GGAATGCCACCCACAGCA	
DUOX1-F	CCCACGTTACCATTTCCATCA	*Duox1*
DUOX1-R	CATCTGCATAGCTGGCTGGA	
DUOX2-F	GGACAGCATGCTTCCAACAAGT	*Duox2*
DUOX2-R	GCCTGATAAACACCGTCAGCA	
NOX1-F	CAGAGCCACTGACATCCTGA	*Nox1*
NOX1-R	CAGACTCGAGTATCGCTGACA	
SAA1-F	GCTACTCACCAGCCTGGTCT	*Saa1*
SAA1-R	GGCCTCTCTTCCATCACTGA	
CCL20-F	GTACTGCTGGCTCACCTCT	*Ccl20*
CCL20-R	CATCTTCTTGACTCTTAGGCTGA	
CXCL1-F	CTGCACCCAAACCGAAGTCAT	*Cxcl1*
CXCL1-R	TTGTCAGAAGCCAGCGTTCAC	
NOS2-F	CTGAACTTGAGCGAGGAGCA	*Nos2*
NOS2-R	GTGCCAGAAGCTGGAACTCT	
IL17a-F	GGACTCTCCACCGCAATGA	*Il17a*
IL17a-R	GGCACTGAGCTTCCCAGATC	
IL17f-F	CCCCATGGGATTACAACATCAC	*Il17f*
IL17f-R	CATTGATGCAGCCTGAGTGTCT	
IL22-F	CCCAGTCAGACAGGTTCCA	*Il22*
IL22-R	TGATCTCTCCACTCTCTCCA	

SFB-specific primers

name	5'-3' sequence	gene
SFB736F [11]	GACGCTGAGGCATGAGAGCAT	16S rDNA
SFB844R [11]	GACGGCACGGATTGTTATTCA	(SFB)
kat-F	GTAGATGGTAACTCGGGAAGTACT	SFBM_1159
kat-R	CTCCCATGGAACGAGCAGTGT	
piplc-F	CCTACTCTAGGAGAAGCAAGAGGA	SFBM_0755
piplc-R	GGTAAAACTCCACCATGACCATTCA	
myoag-F	GTGGTGGCTGGGATATGTGGA	SFBM_0327

myoag-R	CACCCGACTAATTGACCCTTAGGT	
fibrobp-F	GCTGGTAGCCATGTTATCCTTGCA	SFBM_0986
fibrobp-R	CCATTCCTGGTTTTGCATGTGGCA	
flic2-F	GGTGTAAGCATCGGGAATATGGGT	SFBM_0642
flic2-R	CAGCTGTGTTATCTGTTGATGCGA	
adprt-F	GCGAGCTTCCCTCATTACAAGG	SFBSU_007G84
adprt-R	ACCATCCTGAATCTTCTCCAACA	

bacteria group-specific primers

name	5'-3' sequence	gene
UniF334 [12]	ACTCCTACGGGAGGCAGCAGT	16S rDNA
UniR514 [12]	ATTACCGCGGCTGCTGGC	(universal)
928F-Firm [12]	TGAAACTYAAAGGAATTGACG	16S rDNA
Firm1040R [12]	ACCATGCACCACCTGTC	(Firmicutes)
798cfbF [12]	CRAACAGGATTAGATACCCT	16s rDNA
cfb967R [12]	GGTAAGGTTCCTCGCGTAT	(Bacteroidetes)
1080γF [12]	TCGTCAGCTCGTGTYGTGA	16S rDNA
γ1202R [12]	CGTAAGGGCCATGATG	(γ-Proteobact.)
Act920F3 [12]	TACGGCCGCAAGGCTA	16S rDNA
Act1200R [12]	TCRTCCCCACCTTCCTCCG	(Actinobacteria)
En-lsu-3F [13]	TGCCGTAACTTCGGGAGAAGGCA	23S rDNA
En-lsu-3'R [13]	TCAAGGACCAGTGTTCAGTGTC	(Enterobacteriaceae)
Ecoli-F [14]	CATGCCGCGTGTATGAAGAA	16S rDNA
Ecoli-R [14]	CGGGTAACGTCAATGAGCAAA	(*E. coli*)

Supplementary Table S16

Genes upregulated in SFB^{mono} (GSE18348) [8] and *Duoxa*$^{-/-}$ mice

(leading edge gene subset corresponding to left panel of Fig. 5D)

	# of genes
up in SFB^{mono} vs GF (>2.5 fold; p<0.05):	56
leading-edge subset (core enrichment):	37

Gene name	Rank in gene list	Duoxa$^{-/-}$ vs wt	Running ES	SFB^{mono} vs GF
1600029D21RIK	0	3.63	0.09	13.15
SAA1	2	2.47	0.15	126.35
IFIT2	5	1.99	0.19	11.78
HEMT1	11	1.84	0.23	6.06
SAA2	13	1.77	0.27	12.96
HK2	21	1.65	0.31	3.82
USP18	29	1.54	0.33	3.30
PLA2G5	33	1.52	0.36	3.95
CXCL9	50	1.45	0.39	3.18
SLC28A2	57	1.41	0.41	3.82
SMPDL3B	69	1.39	0.43	5.11
ZBP1	83	1.36	0.45	6.73
SLC6A14	98	1.34	0.47	21.29
TIFA	104	1.33	0.49	3.69
NOS2	107	1.33	0.51	6.61
IGTP	125	1.31	0.52	5.92
CASP4	129	1.30	0.54	2.91
LY6D	154	1.29	0.56	4.59
CCL28	236	1.24	0.56	2.98
STOM	246	1.24	0.58	3.24
CEBPD	254	1.24	0.59	3.20
GBP6	268	1.23	0.61	2.64
DMBT1	290	1.23	0.62	3.13
BHMT	336	1.21	0.63	4.80
NFKBIZ	378	1.21	0.64	3.76
PTK6	381	1.21	0.65	3.38
MPA2L	421	1.20	0.66	3.17
IIGP2	440	1.20	0.67	4.10
TGM2	454	1.19	0.68	3.06
SOCS3	593	1.18	0.68	4.52
MAL	642	1.17	0.69	4.26
UPP1	720	1.16	0.69	4.14
PSMB8	844	1.15	0.69	3.75
GZMB	858	1.15	0.70	9.68
TCRB-J	1090	1.14	0.69	2.60
CD38	1113	1.14	0.70	6.08
SERPINA3G	1180	1.13	0.70	2.88

Supplementary Table S17

Genes downregulated in SFB^{mono} (GSE18348) [8] and *Duoxa*$^{-/-}$ mice
(leading edge gene subset corresponding to right panel of Fig. 5D)

	# of genes
down in SFB^{mono} vs GF (>0.6 fold; p<0.05):	65
leading-edge subset (core enrichment):	20

Gene name	Rank in gene list	Duoxa$^{-/-}$ vs wt	Running ES	SFB^{mono} vs GF
SLC5A4A	13782	0.59	0.00	0.33
SLC5A4B	13779	0.65	-0.06	0.35
1300013J15RIK	13776	0.68	-0.11	0.49
FMO5	13775	0.68	-0.16	0.34
SLC7A8	13772	0.70	-0.20	0.41
VMD2L1	13761	0.72	-0.24	0.41
FABP1	13694	0.77	-0.28	0.54
ACY1	13687	0.77	-0.31	0.51
2810439F02RIK	13666	0.78	-0.33	0.46
AQP7	13606	0.80	-0.36	0.36
BC089597	13552	0.81	-0.38	0.23
VWA1	13538	0.81	-0.40	0.51
CYP3A11	13505	0.82	-0.43	0.27
ARG2	13494	0.82	-0.45	0.46
CYP2D26	13464	0.82	-0.47	0.54
C1QDC2	13463	0.82	-0.49	0.52
SPSB4	13423	0.83	-0.51	0.48
PLOD2	13165	0.85	-0.51	0.43
DNMT2	13019	0.86	-0.52	0.44
FBP1	12989	0.86	-0.54	0.42

Supplementary Table S18

Genes upregulated in B6-Jax cohoused with B6-Tac (GSE18348) [8]

and in *Duoxa*$^{-/-}$ mice

(leading edge gene subset corresponding to left panel of Fig. 5E)

	# of genes
up in Jax(+Tac) vs Jax (>2.5 fold; p<0.05):	71
leading-edge subset (core enrichment):	46

Gene name	Rank in gene list	Duoxa$^{-/-}$ vs wt	Running ES	Jax(+Tac) vs Jax
Plet1	0	3.63	0.07	77.30
SAA1	2	2.47	0.12	28.04
RETNLB	4	2.06	0.16	46.51
UBD	10	1.85	0.20	5.21
HEMT1	11	1.84	0.23	19.74
SAA2	13	1.77	0.26	11.07
FUT2	20	1.66	0.29	13.80
HK2	21	1.65	0.32	5.15
SLFN4	24	1.60	0.34	2.66
PLA2G5	33	1.52	0.36	10.10
SAA3	40	1.49	0.39	3.06
CEACAM10	48	1.45	0.41	3.10
CXCL9	50	1.45	0.43	3.58
SMPDL3B	69	1.39	0.44	2.96
IIGP1	79	1.38	0.46	2.55
ZBP1	83	1.36	0.48	3.08
ADM	86	1.36	0.50	2.89
SLC6A14	98	1.34	0.51	3.24
TIFA	104	1.33	0.53	4.33
NOS2	107	1.33	0.54	8.23
IGK-V32	116	1.32	0.56	4.33
TAT	117	1.32	0.57	8.79
LY6D	154	1.29	0.58	3.69
MYL7	161	1.29	0.60	2.70
SLC5A9	178	1.27	0.61	2.87
LY6A	183	1.27	0.62	3.43
CD177	225	1.25	0.63	4.63
STEAP1	243	1.24	0.64	4.85
STOM	246	1.24	0.65	4.18
CEBPD	254	1.24	0.66	3.44
DMBT1	290	1.23	0.67	3.17
BHMT	336	1.21	0.68	5.10
PTK6	381	1.21	0.69	2.61
TGM2	454	1.19	0.69	3.29
MUC4	473	1.19	0.70	2.60
SOCS3	593	1.18	0.70	8.16

IL18	601	1.17	0.71	4.31
MAL	642	1.17	0.72	5.35
UPP1	720	1.16	0.72	2.65
AQP4	787	1.16	0.72	6.52
GZMB	858	1.15	0.72	3.83
CD38	1113	1.14	0.71	5.14
SERPINA3G	1180	1.13	0.71	3.27
PFKFB3	1196	1.13	0.72	6.41
RDH16	1198	1.13	0.73	2.66
CCND1	1243	1.13	0.73	2.56

Supplementary Table S19

Genes downregulated in B6-Jax cohoused with B6-Tac (GSE18348) [8]

and in *Duoxa*$^{-/-}$ mice

(leading edge gene subset corresponding to right panel of Fig. 5E)

	# of genes
down in Jax(+Tac) vs Jax (<0.5 fold; p<0.05):	141
leading-edge subset (core enrichment):	70

Gene name	Rank in gene list	Duoxa$^{-/-}$ vs wt	Running ES	Jax(+Tac) vs Jax
SUSD2	13787	0.56	0.00	0.37
SLC5A4A	13782	0.59	-0.03	0.28
SLC5A4B	13779	0.65	-0.06	0.44
1300013J15RIK	13776	0.68	-0.08	0.23
FMO5	13775	0.68	-0.10	0.21
PCK1	13774	0.68	-0.12	0.20
TREH	13757	0.73	-0.14	0.42
CYP27A1	13754	0.73	-0.16	0.38
OPLAH	13726	0.75	-0.17	0.44
CES1	13699	0.76	-0.19	0.27
FABP1	13694	0.77	-0.20	0.34
BMP8B	13693	0.77	-0.22	0.37
METTL7A	13682	0.77	-0.23	0.35
AI451617	13675	0.78	-0.24	0.41
BC021608	13673	0.78	-0.26	0.26
2810439F02RIK	13666	0.78	-0.27	0.31
CUBN	13660	0.79	-0.28	0.20
BST1	13627	0.79	-0.29	0.36
AQP7	13606	0.80	-0.30	0.19
SULT1A1	13561	0.81	-0.31	0.36
BC089597	13552	0.81	-0.32	0.44
VWA1	13538	0.81	-0.33	0.30
SLC5A11	13508	0.82	-0.34	0.30
CYP3A11	13505	0.82	-0.35	0.05
ARG2	13494	0.82	-0.36	0.22
SLC6A20A	13489	0.82	-0.37	0.26
SELENBP1	13465	0.82	-0.38	0.34
CYP2D26	13464	0.82	-0.39	0.18
C1QDC2	13463	0.82	-0.40	0.40
CAT	13434	0.83	-0.41	0.84
SPSB4	13423	0.83	-0.42	0.40
ABCC2	13390	0.83	-0.43	0.19
C920025E04RIK	13384	0.83	-0.44	0.31
OSBPL1A	13378	0.83	-0.45	0.43
SLC22A4	13369	0.84	-0.46	0.41
EPHX2	13335	0.84	-0.46	0.38

CYP3A25	13330	0.84	-0.47	0.20
PDZK1	13258	0.84	-0.48	0.24
ALDH1A7	13229	0.85	-0.48	0.44
CML5	13209	0.85	-0.49	0.37
PLOD2	13165	0.85	-0.50	0.27
GPR172B	13156	0.85	-0.51	0.44
TSPAN5	13133	0.85	-0.51	0.39
CBR1	13096	0.86	-0.52	0.42
METTL7A	13026	0.86	-0.52	0.41
DNMT2	13019	0.86	-0.53	0.43
FBP1	12989	0.86	-0.54	0.29
EHHADH	12924	0.87	-0.54	0.41
TBC1D24	12893	0.87	-0.54	0.36
GUCA2B	12878	0.87	-0.55	0.39
TMEM43	12876	0.87	-0.56	0.41
TYKI	12851	0.87	-0.56	0.23
NR1D2	12834	0.87	-0.57	0.43
CYP4V3	12694	0.88	-0.57	0.18
HEXB	12653	0.88	-0.57	0.39
MME	12599	0.88	-0.57	0.14
AW491445	12459	0.89	-0.57	0.25
UGT2B5	12445	0.89	-0.58	0.25
PPARGC1A	12443	0.89	-0.58	0.29
RDH7	12413	0.89	-0.59	0.09
CYP3A44	12386	0.89	-0.59	0.32
HSD17B4	12378	0.89	-0.60	0.42
ANGPTL4	12284	0.89	-0.60	0.21
BMP1	12183	0.90	-0.60	0.43
CYP4B1	12051	0.90	-0.59	0.35
APOC3	11983	0.90	-0.59	0.23
THRSP	11886	0.91	-0.59	0.42
SLC5A6	11827	0.91	-0.59	0.38
MMP15	11803	0.91	-0.59	0.44
0610009A07RIK	11795	0.91	-0.60	0.39

Supplementary Table S20

Genes upregulated in cCD (Ref. 9, Tbl. S10) and *Duoxa*$^{-/-}$ mice

(leading edge gene subset corresponding to upper panel of Fig. 6C)

	# of genes
upregulated in cCD vs Ctrl:	287
with expression data for mouse homolog:	172
leading-edge subset (core enrichment):	53

Gene name	Rank in gene list	Duoxa$^{-/-}$ vs wt	Running ES	cCD vs Ctrl
ST3GAL4	0	2.55	0.04	2.12
SAA1	1	2.47	0.08	5.82
IL1RL1	2	2.30	0.11	1.65
IFI44	6	1.87	0.14	1.54
SAA2	12	1.77	0.16	5.98
MMP3	13	1.76	0.19	15.13
S100A9	15	1.68	0.21	6.04
HK2	19	1.65	0.23	2.75
AREG	20	1.64	0.25	2.26
TLR2	23	1.58	0.27	1.94
S100A8	24	1.55	0.29	8.62
CXCL10	27	1.54	0.31	4.24
TLR4	29	1.53	0.32	1.73
CXCL1	35	1.50	0.34	3.63
IL1B	43	1.45	0.36	6.42
CXCL9	46	1.45	0.37	4.53
CXCL11	50	1.42	0.39	4.94
CXCL5	64	1.39	0.40	9.24
CA1	68	1.38	0.41	2.81
ZBP1	74	1.36	0.42	1.87
ADM	77	1.36	0.44	2.05
SLC6A14	88	1.34	0.45	7.32
TIFA	94	1.33	0.46	1.57
LY6D	135	1.29	0.47	2.70
CD177	194	1.25	0.47	4.69
SLAMF7	203	1.24	0.48	1.88
CCL28	204	1.24	0.49	2.34
STEAP1	210	1.24	0.50	1.99
MTHFD2	222	1.24	0.51	1.63
DMBT1	244	1.23	0.51	2.16
MSR1	268	1.22	0.52	1.70
ADAMTS1	296	1.21	0.52	1.71
ANXA3	304	1.21	0.53	1.66
NFKBIZ	315	1.21	0.54	2.33
STEAP4	347	1.20	0.54	2.18

TGM2	374	1.19	0.55	1.89
MUC4	391	1.19	0.56	5.30
TNFRSF17	405	1.19	0.56	1.60
DUSP6	472	1.18	0.56	1.57
STAT1	542	1.17	0.56	2.36
CD274	548	1.17	0.57	2.31
GBP1	555	1.17	0.57	2.57
NPL	686	1.15	0.57	1.57
CH25H	723	1.15	0.57	1.71
PTGFR	724	1.15	0.58	1.52
CD86	772	1.15	0.58	1.62
CYP7B1	776	1.15	0.58	1.85
CCR1	782	1.15	0.59	1.73
MMP10	809	1.14	0.59	9.42
KCNE3	883	1.14	0.59	1.70
CD38	897	1.14	0.60	1.76
LCP2	918	1.13	0.60	1.50
GBP4	961	1.13	0.60	1.91

Supplementary Table S21

Genes downregulated in ileum of cCD patients [9] and *Duoxa*$^{-/-}$ mice
(leading edge gene subset corresponding to lower panel of Fig. 6C)

	# of genes
downregulated in cCD vs Ctrl:	285
with expression data for mouse homolog:	163
leading-edge subset (core enrichment):	72

Gene name	Rank in gene list	Duoxa-/- vs wt	Running ES	cCD vs Ctrl
SUSD2	11293	0.56	0.00	0.34
SLC2A2	11286	0.66	-0.03	0.36
FMO5	11284	0.68	-0.06	0.53
PCK1	11283	0.68	-0.08	0.36
TREH	11268	0.73	-0.10	0.30
PDK2	11267	0.73	-0.12	0.62
HMGCS2	11261	0.73	-0.14	0.27
XPNPEP2	11260	0.73	-0.15	0.26
REEP6	11252	0.75	-0.17	0.31
LEAP2	11232	0.76	-0.19	0.44
ACE	11225	0.76	-0.20	0.45
ESPN	11216	0.77	-0.22	0.57
ACY1	11208	0.77	-0.23	0.62
OSR2	11207	0.77	-0.25	0.60
ANPEP	11186	0.79	-0.26	0.48
AQP1	11154	0.80	-0.27	0.63
CD8B	11139	0.80	-0.28	0.55
AQP7	11137	0.80	-0.30	0.31
METTL7B	11124	0.80	-0.31	0.59
DBP	11121	0.80	-0.32	0.60
SLC5A11	11050	0.82	-0.33	0.33
SEMA6C	11044	0.82	-0.34	0.67
SLC15A1	11036	0.82	-0.35	0.36
CYP2S1	11017	0.82	-0.36	0.57
SLC13A2	10964	0.83	-0.37	0.36
SLC13A1	10919	0.84	-0.37	0.29
EPHX2	10898	0.84	-0.38	0.61
SULT2B1	10874	0.84	-0.39	0.50
GGT1	10871	0.84	-0.40	0.60
HTR1D	10863	0.84	-0.41	0.37
PDZK1	10832	0.84	-0.42	0.36
SOAT2	10820	0.85	-0.42	0.20
ABP1	10793	0.85	-0.43	0.58
SI	10745	0.85	-0.44	0.46
ABCG8	10732	0.85	-0.45	0.50
TM6SF2	10701	0.85	-0.45	0.36

GAL3ST1	10680	0.86	-0.46	0.40
SLC9A3R1	10677	0.86	-0.47	0.62
SLC39A4	10676	0.86	-0.48	0.53
BCAN	10668	0.86	-0.49	0.63
FBP1	10593	0.86	-0.49	0.49
DNASE1	10549	0.87	-0.49	0.39
ACOX2	10537	0.87	-0.50	0.57
ITIH3	10534	0.87	-0.51	0.31
KHK	10216	0.88	-0.49	0.38
GPD1	10195	0.88	-0.49	0.42
CHAD	10179	0.89	-0.50	0.45
SLC6A4	10168	0.89	-0.50	0.27
DAK	10158	0.89	-0.51	0.59
DPEP1	10007	0.89	-0.50	0.31
CLDN15	9983	0.89	-0.51	0.53
MLXIPL	9953	0.90	-0.51	0.48
PKLR	9936	0.90	-0.52	0.30
AMN	9892	0.90	-0.52	0.44
GP2	9859	0.90	-0.52	0.39
NPY	9855	0.90	-0.53	0.32
APOC3	9742	0.90	-0.53	0.23
PHYH	9734	0.90	-0.53	0.56
SFRP5	9666	0.91	-0.53	0.24
DGAT1	9578	0.91	-0.53	0.60
C6	9536	0.91	-0.53	0.21
KLKB1	9518	0.91	-0.53	0.52
TM4SF5	9511	0.91	-0.54	0.37
ASPA	9433	0.91	-0.54	0.47
SLC22A5	9422	0.92	-0.54	0.58
MEP1A	9252	0.92	-0.53	0.50
FGFR3	9235	0.92	-0.53	0.65
RDH5	9203	0.92	-0.54	0.64
LCT	9181	0.92	-0.54	0.19
NR1I3	9081	0.93	-0.54	0.42
HSD3B1	9079	0.93	-0.54	0.30
RGS11	9070	0.93	-0.54	0.59